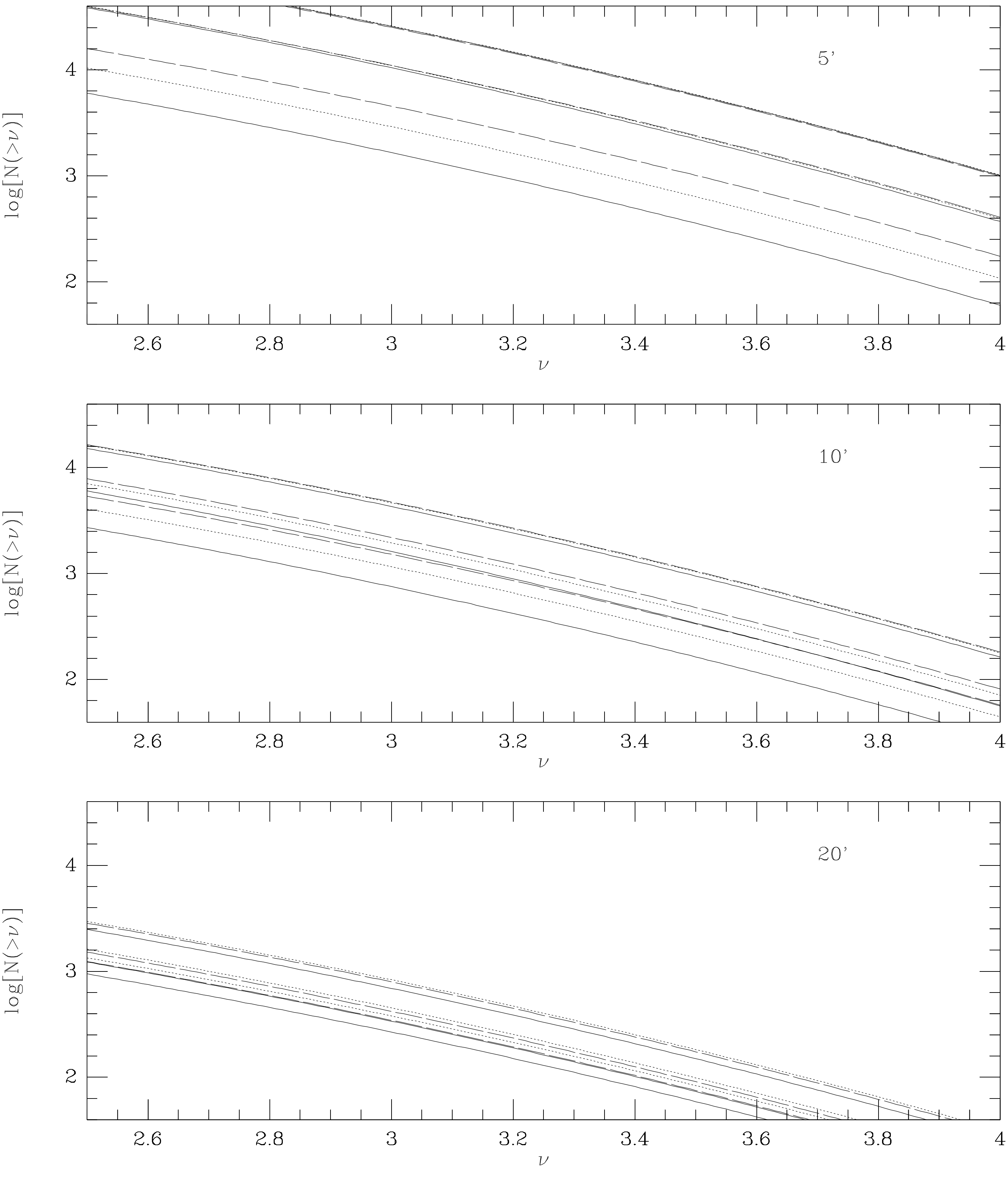
5'
10'
20'
log[N(>ν)]
ν
2
3
4
2.6
2.8
3
3.2
3.4
3.6
3.8
4

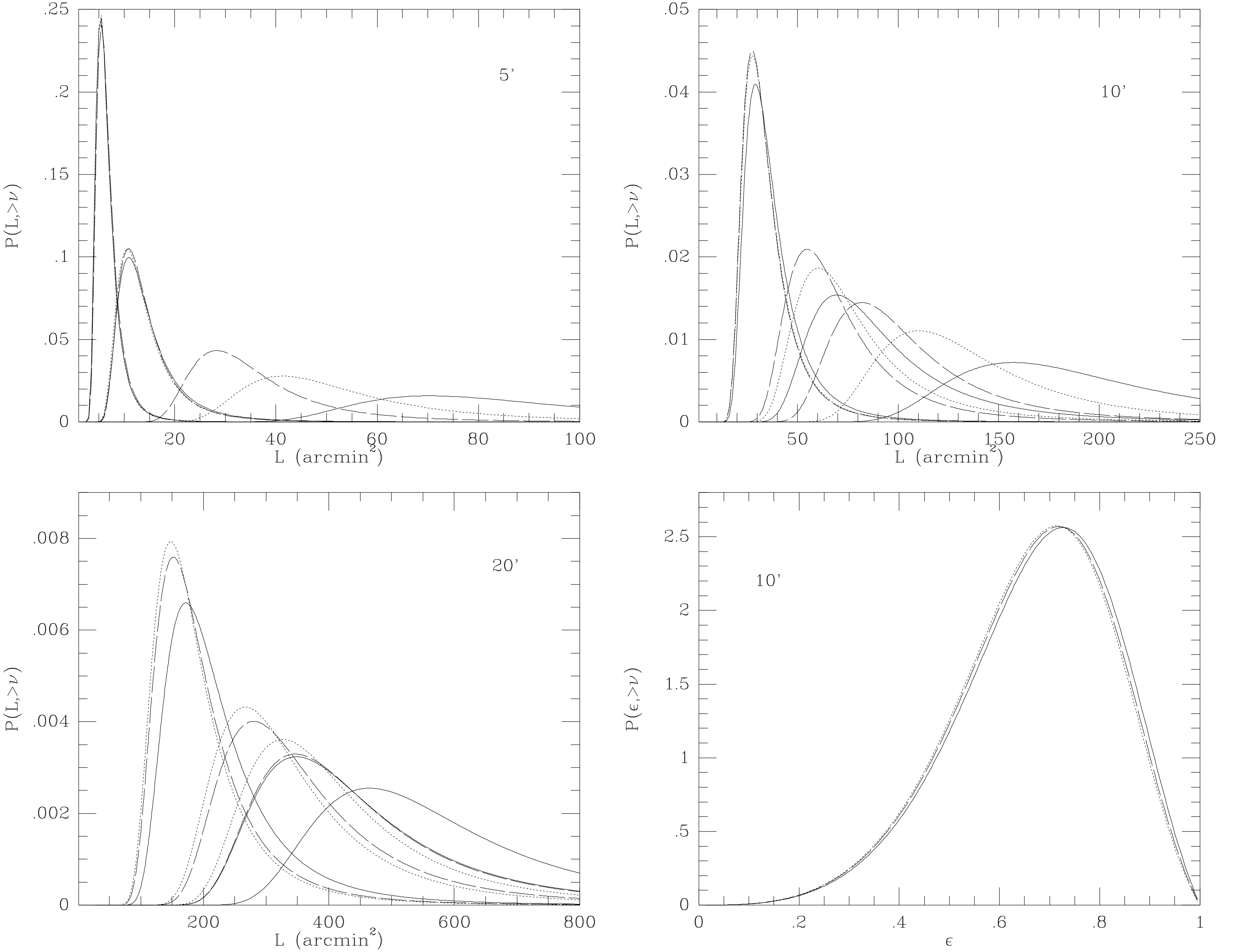
5'
P(L,>ν)
L (arcmin²)
10'
P(L,>ν)
L (arcmin²)
20'
P(L,>ν)
L (arcmin²)
10'
P(ε,>ν)
ε

Peaks in the Cosmic Microwave Background: flat versus open models

R. B. Barreiro[1], J. L. Sanz, E. Martínez-González

Instituto de Física de Cantabria, CSIC-Universidad de Cantabria,

Facultad de Ciencias, Avda. Los Castros s/n, 39005 Santander, Spain

and

L. Cayón, Joseph Silk

Astronomy Department and Center for Particle Astrophysics,

University of California, Berkeley, CA 94720

Received ______________________; accepted ______________________

[1]Dpto. de Física Moderna, Universidad de Cantabria, Facultad de Ciencias, Avda. Los Castros s/n, 39005 Santander, Spain

ABSTRACT

We present properties of the peaks (maxima) of the microwave background anisotropies expected in flat and open cold dark matter models. We obtain analytical expressions of several topological descriptors: mean number of maxima and the probabilty distribution of the gaussian curvature and the eccentricity of the peaks. These quantities are calculated as functions of the radiation power spectrum, assuming a gaussian distribution of temperature anisotropies. We present results for angular resolutions ranging from $5'$ to $20'$ (antenna FWHM), scales that are relevant for the MAP and COBRAS/SAMBA space missions and the ground-based interferometer experiments. Our analysis also includes the effects of noise. We find that the number of peaks can discriminate between standard CDM models, and that the gaussian curvature distribution provides a useful test for these various models, whereas the eccentricity distribution can not distinguish between them.

Subject headings: cosmology: cosmic microwave background—anisotropies: peaks

1. Introduction

The standard way to study the microwave background anisotropies (CMB) is based on the computation of the radiation power spectrum, i.e., the $C_\ell' s$. The texture of the CMB offers a useful alternative to this approach and can be used to test models of galaxy formation. Let us consider the excursions of a gaussian random field above a certain threshold $\nu = (\Delta T)/(\Delta T)_{rms}$. It is of interest to remark that once ν is fixed, all the topological quantities we will calculate are normalization–independent. Earlier work on the properties of peaks in one-dimensional scans and 2D maps of the CMB are due to Zabotin & Nasel'skii (1985) and Sazhin (1985), respectively. A key paper on two-dimensional fields and its implications for the CMB is that of Bond & Efstathiou (1987). This technique was applied to calculate the number of spots on small angular scales in different models (Vittorio & Juszkiewicz 1987; Martínez-González and Sanz 1989) and to study the Tenerife experiment (Gutiérrez et al. 1994). A similar analysis applied to non-gaussian random fields have been performed by Coles & Barrow (1987).

In this Paper, we consider the statistical properties of the CMB, assuming that the temperature fluctuations can be represented by a two-dimensional gaussian random field. The local description of maxima is presented in §2. We will restrict our analysis to the peaks of the field above a certain threshold. In particular we are interested in the following quantities: mean number of peaks over the whole celestial sphere $N(>\nu)$ (§3), gaussian curvature probability density function (p.d.f.) $p(\kappa, >\nu)$ (§4) and eccentricity p.d.f. $p(\epsilon, >\nu)$ (§5). All of them can be calculated analytically in terms of parameters that are related to the CMB radiation power spectrum. This power spectrum is characterized by the Doppler peaks and a cut-off at high ℓ, which depend on the cosmological parameters (for a recent review see Hu 1996). An accurate determination of the radiation power spectrum requires detailed numerical calculations in perturbation theory (Sugiyama 1996). Flat and open cold

dark matter models with a Harrison-Zel'dovich initial power spectrum will be considered. Our analysis includes an angular resolution ranging from $5'$ to $20'$, of interest for future experiments, and also the effects of noise. Conclusions are presented in §6.

2. Local description of maxima

The local description of maxima involves the second derivatives of the field along the two principal directions. As usual, the curvature radii are defined by: $R_1 = [-\Delta_1''(max)/2]^{-1/2}$ and $R_2 = [-\Delta_2''(max)/2]^{-1/2}$, where Δ is the temperature field normalized to the rms-fluctuations. Then with any maximum, we can associate two invariant quantities: the gaussian curvature κ and the eccentricity ϵ given by

$$\kappa = \frac{1}{R_1 R_2}, \quad \epsilon = \left[1 - \left(\frac{R_2}{R_1}\right)^2\right]^{1/2}. \tag{1}$$

The number density of peaks of a two-dimensional homogeneous and isotropic gaussian random field has been studied by Longuet-Higgins (1957) and Bond and Efstathiou (1987). After a straightforward calculation, one can obtain the mean number of maxima (over the celestial sphere) $N(\kappa, \epsilon, \nu) d\kappa\, d\epsilon\, d\nu$ with gaussian curvature, eccentricity and threshold between $(\kappa, \kappa + d\kappa)$, $(\epsilon, \epsilon + d\epsilon)$ and $(\nu, \nu + d\nu)$, respectively. N is given in terms of two spectral parameters γ and θ_* that charaterize the intrinsic cosmological model plus the noise

$$\theta_c = 2^{1/2}\frac{\sigma_0}{\sigma_1}, \quad \gamma = \frac{\sigma_1^2}{\sigma_0\sigma_2}, \quad \theta_* = 2^{1/2}\frac{\sigma_1}{\sigma_2}, \quad \theta_* = \gamma\theta_c, \tag{2}$$

$$\sigma_0^2 = C(0, \sigma), \quad \sigma_1^2 = -2\, C''(0, \sigma), \quad \sigma_2^2 = \frac{8}{3}\, C^{(iv)}(0, \sigma), \tag{3}$$

where σ is the gaussian dispersion ($\sigma = 0.425 \times FWHM$). The C_ℓ's have two different

contributions: the intrinsic cosmological signal and the noise. We will consider flat and open CDM models ($\Omega = 1, 0.3, 0.1$, baryon content $\Omega_b = 0.05$, Hubble constant $h = 0.5$) with adiabatic fluctuations and a Harrison-Zel'dovich primordial spectrum, kindly provided by N. Sugiyama. The C_ℓ's have been normalized to the COBE 2-year maps (Cayón et al. 1996. This normalization does not appreciably change with the 4-year data). We consider several noise amplitudes assuming that all scales contribute at the same level (white noise). The multipole coefficients of the noise $C_{(N)}$ are therefore given by:

$$C_{(N)} = A^2_{(N)}(10') \frac{4\pi}{\sum_\ell (2\ell+1) e^{-\ell(\ell+1)\sigma^2}} \quad . \tag{4}$$

The noise amplitude $A_{(N)}(10')$, i.e. the noise after smoothing with a $10'$ FWHM gaussian window, is fixed at $A_{(N)}(10') = (0, 1, 3) \times 10^{-5}$ with $\sigma = 0.425 \times 10'$, giving $C_{(N)} = (0, 1.9, 17) \times 10^{-15}$ for the three noise levels used in our examples (a justification will be given below). Then, $A_{(N)}$ for other angular resolutions ($5'$,$20'$) can be obtained using the same $C_{(N)}$ through the previous formula.

Following standard observational procedures, we will filter signal plus noise with a gaussian with approximately the same width than the antenna FWHM. The angular correlation function $C(\alpha, \sigma)$ is therefore given by

$$C(\alpha, \sigma) = \frac{1}{4\pi} \sum_\ell (2\ell+1) \left(C_\ell e^{-\ell(\ell+1)\sigma^2} + C_{(N)} \right) P_\ell(\cos\alpha) e^{-\ell(\ell+1)\sigma^2}, \tag{5}$$

In Table 1 we give the coherence length and the parameters γ and θ_* for $\Omega = 0.1, 0.3, 1$, different angular resolutions and $A_{(N)}(10')$'s. θ_* increases with beam size and decreases with $A_{(N)}(10')$. When no noise is present the coherence angle has a range between $8'.6$ and $35'.9$ for the values of the parameters considered. That range decreases as the noise level increases.

We will analyse 2D temperature fluctuations (signal plus noise) with angular resolution $FWHM(') = 5, 10$ and 20, which are of interest for the most sensitive bolometers and radiometers of future space experiments (COBRAS/SAMBA and MAP) and also for the VSA experiment as well as other interferometric experiments. The values of $A_{(N)}(10')$ considered in this paper cover the range of sensitivities expected for the future experiments. In particular, the best expected sensitivity of COBRAS/SAMBA corresponds, in practice, to the case $A_{(N)}(10') = 0$.

3. Number of peaks

The number of peaks above the threshold ν, $N(>\nu)$, can be calculated from the differential number $N(\nu)d\nu$

$$\begin{aligned} N(\nu) &= N_T \left(\frac{6}{\pi}\right)^{1/2} e^{-\nu^2/2} \left[\gamma^2\left(\nu^2-1\right)\left(1-\frac{1}{2}\mathrm{erfc}(\gamma\nu s)\right)+\right. \\ &\left. \nu\gamma\left(1-\gamma^2\right)\frac{s}{\pi^{1/2}}e^{-\gamma^2\nu^2 s^2} + t\left(1-\frac{1}{2}\mathrm{erfc}(\gamma\nu s t)\right)e^{-\gamma^2\nu^2 t^2}\right], \end{aligned} \tag{6}$$

$$s = \left[2\left(1-\gamma^2\right)\right]^{-1/2}, \quad t = \left(3-2\gamma^2\right)^{-1/2} \tag{7}$$

and $N_T = \left(3^{1/2}{\theta_*}^2\right)^{-1}$ is the total number of peaks over the whole celestial sphere.

In Figure 1, we show the cumulative number of peaks for different values of Ω and $A_{(N)}(10')$. Generically, the number of peaks increases if we decrease either the beam size or the Ω parameter, except for $FWHM = 5'$ with $A_{(N)}(10') = 3 \times 10^{-5}$ and $FWHM = 20'$ where the number is greater for $\Omega = 0.3$. For a noiseless map (i.e. $A_{(N)}(10') = 0$) and angular resolution of $5'$, the number of peaks above the threshold $\nu = 3$ for $\Omega = 0.1$ is approximately 3 times the value for $\Omega = 1$ (i.e. 4541 as compared to 1657 peaks for the

open and flat cases, respectively). However, when noise is present, the most favourable case is an angular resolution of $10'$, at which the noise decreases considerably while the signal is slightly affected. In fact, using a χ^2 test and assuming Poissonian errors, the hypothesis that the flat and open models are derived from the same population is rejected at a confidence level $\gtrsim 99\%$ except for an angular resolution of $5'$, $A_{(N)}(10') = 3 \times 10^{-5}$ and $\Omega = 0.3$. Moreover, as previously indicated, the best confidence level is attained at the $10'$ angular resolution. Since we are considering very small angular scales, the cosmic variance will not affect our results from the practical point of view.

On the other hand, we may ask whether gravitational lensing can change these results. An estimate of the coherence length including, or not including, lensing leads to $(\theta_c^{gl}/\theta_c)^2 \simeq 1 - a^2$, with $a \equiv (\sigma(\beta)/\beta)_{\beta=0}$ being the relative bending dispersion at zero lag. For standard CDM and low-Ω CDM models: $a \lesssim 0.18$, so the number of maxima (which at high thresholds is approximately proportional to the coherence length) is only slightly modified, i.e. $\lesssim 3\%$ (Martínez-González, Sanz and Cayón 1996).

In Table 2, we give the number of peaks above the thresholds $\nu = 3, 3.5, 4$ for different values of Ω, angular resolutions and levels of $A_{(N)}(10')$.

An equivalent quantity that can be used is the mean area of the peaks above a certain threshold (defined as the total area above that threshold divided by the corresponding number of peaks). The behaviour of this quantity can be easily obtained from the number of peaks and so it does not incorporate any new information that discriminates between the different models. As an example, for the case of FWHM=$10'$, $\nu = 3$ and $A_{(N)}(10') = 3 \times 10^{-5}$, we find a mean area ($arcmin^2$) of 42.4 for $\Omega = 0.1$ and 46.7 for Ω=1, whereas for the $A_{(N)}(10') = 0$ these values increase to 132.0 and 266.1, respectively.

4. The distribution of gaussian curvature

The distribution of peaks above the threshold ν with inverse of the gaussian curvature $L \equiv \kappa^{-1}$ between $(L, L + dL)$, $p(L, > \nu)$, can be obtained from the following p.d.f.

$$p(L,\nu) = \left(\frac{6}{\pi}\right)^{1/2} a^4 t L^{-5} e^{a^2 L^{-2}} e^{-\frac{3}{2}t^2\nu^2} \mathrm{erfc}\left[\frac{s}{t}\left(aL^{-1} - \gamma\nu t^2\right)\right], \tag{8}$$

$$a = 2\gamma{\theta_c}^2 \tag{9}$$

In Figure 2, we represent the p.d.f $p(L, > \nu)$ for different angular resolutions (FWHM($'$) $= 5, 10, 20$) and threshold $\nu = 3$. In all the cases, except when the beam size is very small ($5'$) and the noise amplitude $A_{(N)}(10')$ high, the curves associated with flat and open models clearly differ. In those cases, using a KS-test, the null hypothesis that the flat and open models are derived from the same population is rejected at a confidence level $\gtrsim 99\%$. The best case is obtained for an angular resolution of $10'$ when noise is present. Increasing the threshold slightly modifies the shape of the distribution: the height of the maximum increases and the curve is shifted to lower L, i.e., the peaks fall more rapidly for higher ν .

On the other hand, we can obtain the mean L for the different models. For the case of FWHM=$10'$ and $A_{(N)}(10') = 3 \times 10^{-5}$, we find (in arcmin^2) $< L >= 36.0$ and 38.7 for $\Omega = 0.1$ and 1, respectively. If we consider the same cases for $A_{(N)}(10') = 0$ the corresponding mean L's are given by 106.9 ($\Omega = 0.1$) and 177.7 ($\Omega = 1$). Then, since the error in $< L >$ due to cosmic variance is expected to be very small for the small angular scales considered, we can also use the mean values of L to distinguish between the flat and open models. In Table 3 the mean L's are given for the models considered.

In order to measure the gaussian curvature from a map obtained by an experiment, the required pixel size would need to be approximately one fifth of the typical curvature

radius of the maxima. The two curvature radii for each peak can be measured by a fit to a paraboloid centered on the maximum temperature. The pixel size should be a compromise between having an appropriate number of pixels to perform the fit and remaining in the vicinity of the maximum. In particular, if we want to test Ω values as low as 0.1 for an angular resolution of $10'$ and $A_{(N)}(10') = 0$ the required size should be $\approx 2'$.

5. The distribution of eccentricities

The distribution of peaks above the threshold ν with eccentricity between $(\epsilon, \epsilon + d\epsilon)$, $p(\epsilon, > \nu)$, can be obtained from the following p.d.f.

$$\begin{aligned} p(\epsilon, \nu) \quad = \quad & \frac{32(6)^{1/2}}{\pi} e^{-\frac{1}{2}\nu^2} \epsilon^3 \frac{(1-\epsilon^2)}{(2-\epsilon^2)^5} \left\langle (H\pi)^{1/2} e^{-G} \left(1 - \frac{1}{2}\mathrm{erfc}(H^{1/2}\gamma\nu s)\right)\right. \\ & [3H^2(1-\gamma^2)^2 + 6H^3\gamma^2(1-\gamma^2)\nu^2 + (H\gamma\nu)^4] + \\ & \left. e^{-s^2\gamma^2\nu^2} s \left(5H^3\gamma(1-\gamma^2)^2\nu + H^4(\gamma\nu)^3(1-\gamma^2)\right)\right\rangle, \end{aligned} \tag{10}$$

$$H = \frac{(2-\epsilon^2)^2}{(3-2\gamma^2)\epsilon^4 + 4(1-\epsilon^2)}, \quad G = H\frac{(\gamma\nu\epsilon^2)^2}{(2-\epsilon^2)^2}. \tag{11}$$

We note that there is an error in the expression given by Bond and Efstathiou(1987) for the conditional probability $P(e|\nu)$, where e is the ellipticity related to ϵ by $\epsilon = 2(e/(1+2e))^{1/2}$. We have studied $p(\epsilon, > \nu)$ for different angular resolutions, noise amplitudes $A_{(N)}(10')$, thresholds and models. The main conclusion is that it would be difficult to distinguish between the cosmological models based on the comparison of eccentricities. As a typical example, in Figure 2, we represent the p.d.f $p(\epsilon, > \nu)$ for the angular resolution of $10'$, threshold $\nu = 3$ and no noise. The introduction of some level of noise clearly makes things worse. Hence we can generically say that the eccentricity p.d.f.

is not a good test for distinguishing between flat and open models. On the other hand, Gurzadyan & Kocharyan (1992, 1993) argue that mixing of photons in a universe with negative curvature will produce elongated shapes as compared to the flat case. All of our results lead to the opposite conclusion: the eccentricity p.d.f. for flat and low-Ω universes show similar bell-shape (for thresholds $\nu = 3, 4$) with mean value $< \epsilon > \approx 0.7$ and almost the same dispersion. Therefore, we conclude that the eccentricity is a bad discriminator of the Ω parameter.

6. Conclusions

We have studied the distribution of peaks above a threshold ν using the mean number and two local quantities: gaussian curvature and eccentricity. We have considered a whole sky coverage, with angular resolutions of $5, 10, 20$ arcmin (antenna FWHM) and different levels of noise $A_{(N)}(10') = (0, 1, 3) \times 10^{-5}$, and we have calculated the distribution of these quantities for flat and open CDM models (with a Harrison-Zel'dovich primordial spectrum). Our main conclusions are that the number of peaks and the gaussian curvature are good discriminators of the geometry of the universe, whereas the eccentricity cannot be used to distinguish between different Ω values. For thresholds $\nu = 3, 4$, these curves are indistinguishable for flat and open models, and we disagree with Gurzadyan & Kocharyan (1992, 1993) who argue that mixing of photons in a space of negative curvature would tend to elongate the spots in the CMB. On the other hand, an angular resolution of $10'$ is the most appropiate to distinguish between low-Ω and flat models when noise is present.

We would like to thank N. Sugiyama for providing us the radiation power spectrum and the referee E.L. Wright for his useful comments. EMG and JLS acknowledge financial support from the Spanish DGICYT, project PB92-0434-C02-02. RBB acknowledges a

Spanish M.E.C. Ph.D. scholarship. JS and LC have been supported in part by a grant from NASA. LC was also supported by a Fullbright Fellowship. We acknowledge financial support from the PECO contract of the EU ERBCIPDCT 940019.

REFERENCES

Bond, J.R. & Efstathiou, G. 1987, MNRAS, 226, 407

Cayón, L., Martínez-González, E., Sanz, J.L., Sugiyama, N. & Torres, S. 1996, MNRAS, 279, 1095.

Coles, P. & Barrow, J.D. 1987,MNRAS, 228, 407

Gurzadyan, V.G. & Kocharyan, A.A. 1992, A&A, 260, 14

Gurzadyan, V.G. & Kocharyan, A.A. 1993, Int. J. Mod. Phys., D2, 1

Gutiérrez, C., Martínez-González, E., Cayón, L., Rebolo, R. & Sanz, J.L. 1994, MNRAS, 271, 553

Hu, W. 1996, in The Universe at High-z, Large-Scale Structure and the Cosmic Microwave Background, ed. E. Martínez-González & J.L. Sanz, Springer-Verlag.

Vittorio, N. & Juszkiewicz, R. 1987, ApJ, 314, L29

Longuet-Higgins, M.S. 1957, Phil.Trans.Roy.Soc.London, A, 249, 321

Martínez-González, E. & Sanz, J.L. 1989, MNRAS, 237, 939

Sazhin, M.V. 1985, MNRAS, 216, 25P

Sugiyama, N. 1996, in Microwave Background Anisotropies, ed. F. Bouchet (Les Arcs), in press

Zabotin, N.A. & Nasel'skii, P.D. 1985, Sov. Astr., 29, 614

This manuscript was prepared with the AAS LaTeX macros v4.0.

Fig. 1.— Logarithm of the number of peaks above a threshold ν versus the threshold, for different angular resolutions. The dashed and dotted lines correspond to open universes (Ω =0.1 and 0.3, respectively) and the solid one to a flat universe. Each set of three different lines corresponds to values of $A_{(N)}(10') = (3, 1, 0) \times 10^{-5}$ (from top to bottom).

Fig. 2.— We plot in three of the figures the distribution of L for peaks above a threshold $\nu = 3$ and several angular resolutions. The first, second and third set of 3 different lines (from left to right) corresponds to values of $A_{(N)}(10') = (3, 1, 0) \times 10^{-5}$, respectively. The p.d.f. p($\epsilon, > \nu$) for a signal-dominated map ($A_{(N)}(10') = 0$), ν =3 and FWHM=$10'$ is shown in the bottom right figure. In the four plots the dashed, dotted and solid lines correspond to the cases Ω =0.1,0.3 and 1, respectively.

Table 1: Coherence angle and γ and θ_* parameters related to the peaks

		$A_{(N)}(10') = 0$			$A_{(N)}(10') = 10^{-5}$			$A_{(N)}(10') = 3 \times 10^{-5}$		
FWHM	Ω	$\theta_c(')$	γ	$\theta_*(')$	$\theta_c(')$	γ	$\theta_*(')$	$\theta_c(')$	γ	$\theta_*(')$
	0.1	8.6	0.53	4.5	5.7	0.44	2.5	3.6	0.61	2.2
$5'$	0.3	11.1	0.45	5.0	5.9	0.40	2.3	3.5	0.61	2.2
	1.0	15.0	0.40	6.1	6.1	0.37	2.3	3.6	0.60	2.1
	0.1	15.0	0.49	7.4	12.8	0.45	5.7	8.4	0.54	4.5
$10'$	0.3	17.0	0.52	8.9	13.7	0.42	5.8	8.5	0.53	4.5
	1.0	22.0	0.43	9.4	16.0	0.34	5.5	8.9	0.50	4.4
	0.1	32.3	0.44	14.2	29.7	0.42	12.3	21.1	0.45	9.6
$20'$	0.3	30.2	0.48	14.6	28.0	0.45	12.7	20.5	0.48	9.7
	1.0	35.9	0.49	17.5	32.9	0.42	13.9	23.0	0.43	9.9

Table 2: Number of peaks above the threshold ν

		$A_{(N)}(10') = 0$			$A_{(N)}(10') = 10^{-5}$			$A_{(N)}(10') = 3 \times 10^{-5}$		
FWHM	ν	Ω=0.1	Ω=0.3	Ω=1	Ω=0.1	Ω=0.3	Ω=1	Ω=0.1	Ω=0.3	Ω=1
	3	4541	2912	1657	11019	10965	10459	25147	25883	25692
$5'$	3.5	1011	636	357	2401	2362	2228	5674	5842	5794
	4	174	108	60	407	397	371	986	1016	1007
	3	1518	1160	753	2192	1953	1615	4727	4660	4295
$10'$	3.5	335	258	164	479	423	341	1055	1038	949
	4	57	44	28	81	72	56	182	179	163
	3	345	379	267	419	452	339	795	832	690
$20'$	3.5	75	84	59	91	99	73	174	183	150
	4	13	14	10	15	17	12	30	31	25

Table 3: $< L >$ $(arcmin^2)$ of the peaks above the threshold $\nu = 3$

	$A_{(N)}(10') = 0$			$A_{(N)}(10') = 10^{-5}$			$A_{(N)}(10') = 3 \times 10^{-5}$		
FWHM	Ω=0.1	Ω=0.3	Ω=1	Ω=0.1	Ω=0.3	Ω=1	Ω=0.1	Ω=0.3	Ω=1
$5'$	37.2	55.3	91.4	14.7	14.5	15.1	7.0	6.8	6.8
$10'$	102.7	126.5	132.7	72.5	79.7	91.4	36.0	36.3	38.6
$20'$	418.3	400.2	485.9	357.7	341.7	420.0	203.1	196.5	230.1